Visualization of the core-scattering dynamics of Rydberg wave packets

J. A. West, and C. R. Stroud, Jr.

The Institute of Optics and Rochester Theory Center for Optical Science and Engineering, University of Rochester, Rochester, New York 14627

west@optics.rochester.edu

Abstract: We present classical and quantum studies of the scattering dynamics of Rydberg electron wave packets from the electronic core of alkali atoms. In quantum systems an ideal state for studying such effects is an angularly localized wave packet in which the primary effect of the scattering is to cause precession. The scattering is enhanced by the application of an external dc electric field. We calculate and animate the field-induced dynamics of both hydrogenic and alkali wave packets and compare them to classical atomic models. We find that in alkali systems the scattered wavefunction can be divided into two components: one whose nearly hydrogenic behavior is due to quantum interference near the core, and another which exhibits the orbital precession found in classical models of nonhydrogenic atoms.

OCIS codes: (020.0020) Atomic and molecular physics, (020.5780) Rydberg states, (020.6580) Stark effect

References

1. M. Nauenburg, C. R. Stroud. Jr. and J. Yeazell, "The classical limit of an atom," Sci. Am. **270**, 24-29 (1994).
2. C. Raman, T. C. Weinacht and P. H. Bucksbaum, "Stark wave packets viewed with half-cycle pulses," Phys. Rev. A , **55**, R3995-R3998 (1997).
3. D. W. Schumacher, B. J. Lyons, and T. F. Gallagher, "Wave packets in perturbed Rydberg systems," Phys. Rev. Lett. , **78**, 4359-4362 (1997).
4. B. Hupper, J. Main, and G. Wunner, "Nonhydrogenic Rydberg atoms in a magnetic field: A rigorous semiclassical approach", Phys. Rev. A , **53**, 744-759 (1966).
5. P. A. Dando, T. S. Monteiro, D. Delande, and K. T. Taylor, "Role of core-scattered closed orbits in nonhydrogenic atoms," Phys. Rev. A , **54**, 127-138 (1996).
6. M. Courtney, N. Spellmeyer, H. Jiao, and D. Kleppner, "Classical, semiclassical and quantum dynamics in the lithium Stark spectra," Phys. Rev. A , **51**, 3604-3620 (1995); M. Courtney and D. Kleppner, "Core-induced chaos in diamagnetic lithium," Phys. Rev. A **53**, 178-191 (1996).
7. J. Yeazell and C. R. Stroud, Jr., "Rydberg-atom wave packets localized in the angular variables," Phys. Rev. A **35**, 2806-2809 (1987); "Observation of spatially localized atomic electron wave packets," Phys. Rev. Lett. , **60**, 1494-1497 (1988).
8. R. Bluhm and V. A. Kostelecky, "Long-term evolution and revival structure of Rydberg wave packets for hydrogen and alkali-metal atoms," Phys. Rev. A , **51**, 4767-86 (1995).
9. J. Gay, D. Delande, and A. Bommier, "Atomic quantum states with maximum localization on classical elliptical orbits," Phys. Rev. A **39**, 6587 (1989).
10. N. Bohr, "On the quantum theory of line spectra," in *Niels Bohr, Collected Works*, edited by J. Nielsen (North-Holland Pub. Co., New York, 1976), Vol. 3.
11. T. P. Hezel, C. E. Burkhardt, M. Ciocca, and J. J. Leventhal, "Classical view of the Stark effect in hydrogen atoms," Am. J. Phys., **60**, 324-328 (1992).
12. A. Hooker, C. H. Greene, and W. Clark, "Classical examination of the Stark effect in hydrogen," Phys. Rev. A , **55**, 4609-4612 (1997).

#1956 - $10.00 US
Received June 25, 1997; Revised July 3, 1997

13. See, for example, R. J. Finkelstein, "Nonrelativistic Mechanics," (W. A. Benjamin, Inc., Reading, MA, 1973) 298.
14. See, for example, H. Goldstein, "Classical Mechanics," (Addison-Wesley, Reading, MA, 1981) 509.
15. T. P. Hezel, C. E. Burkhardt, M. Ciocca, and J. J. Leventhal, "Classical view of the properties of Rydberg atoms: Application of the correspondence principle," Am. J. Phys., **60**, 329-335 (1992).
16. J. Pascale, R. E. Olson and C.O. Reinhold, "State-selective capture in collisions between ions and ground- and excited-state alkali-metal atoms," Phys. Rev. A **42**, 5305-5314 (1990).
17. J. N. Bardsley, "Pseudopotentials in atomic and molecular physics," Case Studies in Atomic Physics, **4** 299-368 (1974).
18. M. L. Zimmerman, M. G. Littman, M. M. Kash, and D. Kleppner, "Stark structure of the Rydberg states of alkali-metal atoms," Phys. Rev. A , **20**, 2251-2275 (1979).

1. Introduction

Although wave packet studies in Rydberg atoms were initially motivated by a desire to explore the classical limit of the hydrogen atom[1], recent work has shown that such wave packets also provide an excellent arena for examining non-hydrogenic effects in multi-electron atoms[2,3]. In atoms with two or more valence electrons, the possibility of exciting multi-electron wave packets is very intriguing and represents a considerable challenge both theoretically and experimentally. But even in atoms with a single valence electron there are interesting multi-electron effects due to the presence of the non-Coulombic core. In this paper we will show that the behavior of wave packet states in such atoms can reveal the classical dynamics underlying scattering from complex cores.

Recent treatments of core scattering in alkali atoms have used a semiclassical analysis of the scaled energy levels to model nonhydrogenic effects in applied fields[4–6]. The aim of these studies was to gain a better understanding of non-integrable quantum systems whose analogs are classically chaotic. The standard semiclassical techniques rely on the summation of contributions from hydrogenic closed orbits and include both Coulomb-scattered and core-scattered orbits. These calculations have provided excellent agreement with the full quantum treatments for both the diamagnetic[4,5] and Stark[6] cases.

Our approach concentrates on the dynamics of the wavefunction instead of the spectrum. By preparing the electron initially in an angularly localized wave packet[7] or elliptic state[1], we can isolate the core scattering effects from the dynamics associated with radial[8] or Stark wave packets[2]. Elliptic states have a strong correspondence with classical theory[9] and this allows us to compare the alkali atom results with the well-known classical and quantum dynamics of the hydrogen atom. With only minor modifications of existing experimental techniques[2,7] it should be possible to very directly examine the dynamics of an individual scattering event.

2. Stark dynamics of elliptic states in hydrogen

We begin with a brief review of the dynamics of a classical hydrogen atom in a dc electric field[10–12]. We will use atomic units throughout the paper. The interesting field-induced dynamics can be separated from the Kepler motion by examining slowly varying orbital parameters such as the angular momentum $\mathbf{L} = \mathbf{r} \times \mathbf{p}$ and the Runge-Lenz vector $\mathbf{A} = \mathbf{p} \times \mathbf{L} - \mathbf{r}/r$. Like the angular momentum, the Runge-Lenz vector is a constant of the field-free motion. It lies antiparallel to the major axis of the orbit and has a magnitude equal to the orbital eccentricity ϵ.

The Hamiltonian for the system including the dc electric field $\mathbf{E}$ is

$$H = \frac{p^2}{2} + V(r) + \mathbf{r} \cdot \mathbf{E}. \tag{1}$$

#1956 - $10.00 US
Received June 25, 1997; Revised July 3, 1997

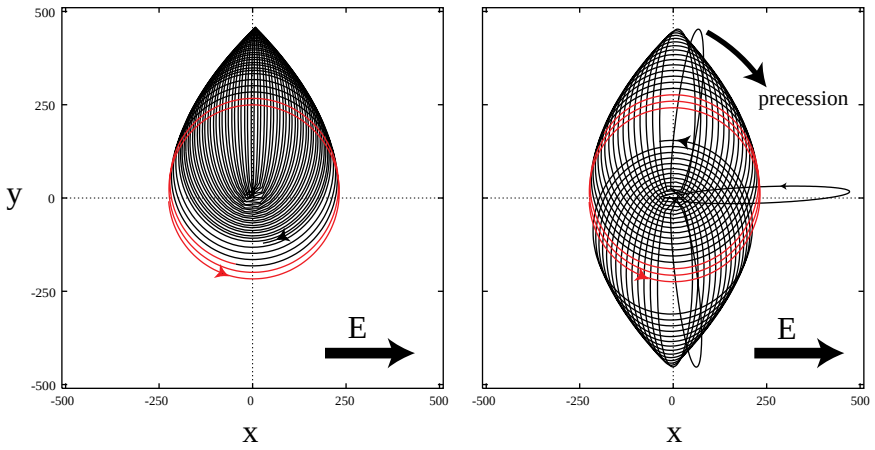

Figure 1: Numerical simulations of a classical electron trajectory showing Stark oscillations in a dc electric field. The electron is initially in a circular orbit in the xy-plane with $n = 15$ and $L_z = |\mathbf{L}| = 15$. An 800 V/cm dc electric field is in the x-direction and the resulting Stark period T_s is approximately 84 Kepler periods. The first few orbits are colored red for clarity and the trajectory is followed for slightly less than half of a Stark period. a) The trajectory for a pure Coulomb potential. The electron backscatters in the linear obit and nearly retraces the original trajectory in the opposite direction. b) The trajectory in the sodium model potential. Note the precession of the highly eccentric orbit.

Choosing $V(r) = -1/r$, the hydrogen Coulomb potential, we can form the equations of motion for $\mathbf{L}$ and $\mathbf{A}$, and average them over a Kepler period T_K. The remaining adiabatic evolution of the averaged classical parameters is given by

$$\begin{aligned} \left\langle \dot{\mathbf{A}} \right\rangle_{T_K} &= \frac{3}{2} \langle \mathbf{L} \rangle_{T_K} \times \mathbf{E}(t), \\ \left\langle \dot{\mathbf{L}} \right\rangle_{T_K} &= \frac{3n^2}{2} \langle \mathbf{A} \rangle_{T_K} \times \mathbf{E}(t), \end{aligned} \tag{2}$$

where n corresponds to the classical field-free energy $\mathcal{E} = -1/(2n^2)$. Although the field does induce a classical Stark shift in the energy (for a recent discussion see Ref. 12) we will focus on the dynamics of the orbit.

Equations (2) are easily solved for a dc electric field in the xy-plane of the classical orbit giving sinusoidal solutions for L_z, A_x and A_y. This analytic result allows us to interpret the orbital deformation in the trajectory shown in Fig. 1a. The frequency of this oscillation is given by the Stark frequency $\omega_s = \frac{3}{2}nE$ and we show the corresponding oscillation of the angular momentum in Fig. 2.

Quantum mechanically we can see identical behavior in the dynamics of an elliptic state in a dc electric field. The analysis of the classical electron interacting with the field did not depend on the exact initial position and momentum, but rather on the initial orbital parameters. The time averages in Eqs. (2) can be replaced by ensemble averages and the results can now be interpreted in terms of an ensemble of electrons rather than in terms of one isolated electron. A quantum-mechanical analog of such a classical ensemble traveling in an elliptic orbit is an elliptic state[9]. Formally an elliptic state is a coherent state of the rotation group in three dimensions, SO(3), whose generators are two components of the scaled Runge-Lenz operator, $n\hat{A}_x$ and $n\hat{A}_y$, and a component of the angular momentum, $\hat{L}_z$. These states can be well-described classically and, although they represent stationary states, the spatial distributions of elliptic

#1956 - $10.00 US
Received June 25, 1997; Revised July 3, 1997

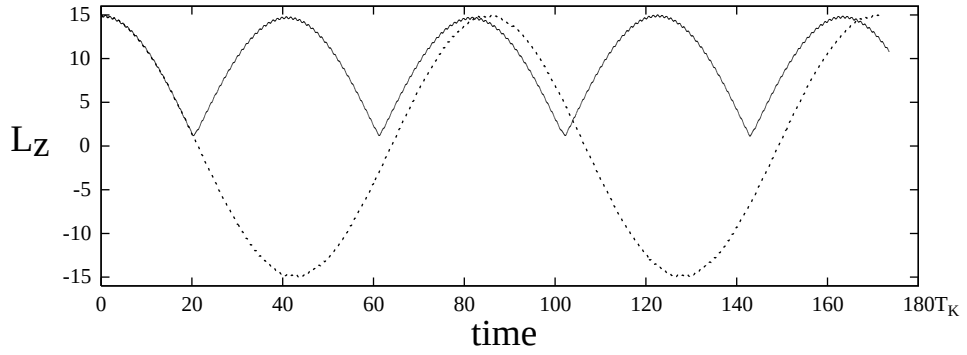

Figure 2: The classical dynamics of the angular momentum for the trajectories shown in Fig. 1. The evolution is followed for two complete Stark periods. The dashed curve is hydrogen and the solid curve is for the sodium model potential. Note that the sodium curve has a shorter Stark period because the scattering occurs at a non-zero value of the angular momentum.

state wavefunctions closely resemble the corresponding classical ellipses. In this paper the dynamics of the wavefunction will result from an external electric field. To avoid confusion we point out that there are *superpositions* of elliptic states from neighboring n manifolds which produce dynamic field-free wave packets known as elliptic orbit wave packets. For the purposes of this paper, we feel that the use of a single elliptic state better illustrates the effect of core scattering.

The circular states $|n, n-1, \pm(n-1)\rangle$ are the only states in a given n manifold which are both elliptic states and field-free eigenstates. The animation in Fig. 3a shows the time evolution of a circular state of hydrogen in a weak dc electric field (manifolds of different n are not mixed). The calculation was performed by integrating Schrödinger's equation in the presence of a dc electric field using hydrogenic dipole moments. The three dimensional probability distribution is projected onto the xy plane. The parameters were chosen to match the classical orbit in Fig. 1. The resulting deformation of the wavefunction is identical to the oscillations of the classical ellipse in Fig. 1a and it can be shown that the wavefunction remains in an elliptic state throughout its evolution. The dynamics of the expectation value of the angular momentum is sinusoidal as shown by the dashed curve in Fig. 4a

3. Stark dynamics of elliptic states in alkali atoms

When non-Coulombic effects are introduced into the potential $V(r)$ the classical Stark dynamics is quite different as shown in Fig 1b. We use a model potential[16] for sodium which includes long range polarizability terms as well as short range core effects

$$V(r) = -\frac{1}{r}[1 + 10(1 + ar + br^2)e^{-cr}] - \frac{1}{2}\alpha_d \frac{r^2}{(r^3 + r_c^3)^2} - \frac{1}{2}\alpha_q' \frac{r^3}{(r^3 + r_c^3)^3}, \qquad (3)$$

where α_d is the dipole core polarizability, α_q' is the dynamical quadrupole polarizability of the core and the parameters a, b, c, and r_c are chosen to match sodium spectroscopic data[16].

It is well-known[13] that additions to the Coulomb core $V(r) = -1/r + \phi(r)$ lead

#1956 - $10.00 US
Received June 25, 1997; Revised July 3, 1997

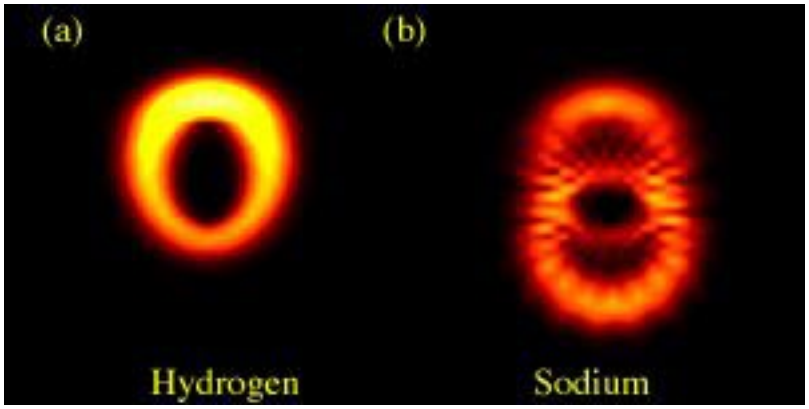

Figure 3: An animation comparing the quantum Stark dynamics in hydrogen and sodium. In both cases the electron is initially in a circular state in the xy plane with $n = 15$ and $\langle L_z \rangle = 14$ with an 800 V/cm dc electric field in the x-direction. a) In hydrogen the quantum behavior is identical to the classical Stark evolution shown in Fig. 1a. b) The behavior in sodium is more complex. Note how part of the wave function behaves hydrogenically while the remainder shows the rapid precession of the non-Coulombic classical orbits in Fig. 1b.

to a precession of the Runge-Lenz vector and hence the major axis of the orbital ellipse

$$\dot{\mathbf{A}} = -\frac{1}{r}\frac{d\phi}{dr}\mathbf{L} \times \mathbf{r}. \tag{4}$$

This precession of the orbit is analogous to the precession caused by perturbations in celestial potentials such as the gravitational correction that leads to the advance of the perihelion of Mercury[14,15]. Under field-free conditions the precession rate of the atomic orbit is constant and for nearly circular orbits it is negligible. However, for highly eccentric orbits, the electron closely approaches the core at its inner turning point causing the orbit to precess. In Fig. 1b we show the effect of this precession on the Stark dynamics[15]. Initially, the behavior is nearly hydrogenic and the orbital parameters begin to vary sinusoidally. However, as the eccentricity increases, the core effects become prominent causing a rapid precession of the orbit. As the highly eccentric orbit precesses its interaction with the field changes and when the orbit has rotated by an angle of nearly 180° the field now causes the magnitude of the angular momentum to increase and the precessional rate becomes negligible once again. This precessional mechanism prevents the angular momentum from changing sign as it does in hydrogen and from the solid curve in Fig. 2 we see that this effect places a lower limit on the angular momentum.

For a field of 800 V/cm the rapid precession occurred in only a few Kepler periods but its duration is inversely proportional to the field strength. In weaker fields the period of rapid precession may last many Kepler periods and the electron undergoes many near-collisions with the core. As we will see in the following quantum mechanical simulations, these multiple scattering events in weak fields produce a larger scattered component in the wavefunction.

Although the long-range polarizability terms in Eqn. 3 do produce nonhydrogenic effects, we find that they are not essential for a qualitative description of the classical dynamics of the electron[17]. It is the short range exponential term that provides the dominant core-scattering effect that we see in Fig. 1b.

#1956 - $10.00 US
Received June 25, 1997; Revised July 3, 1997

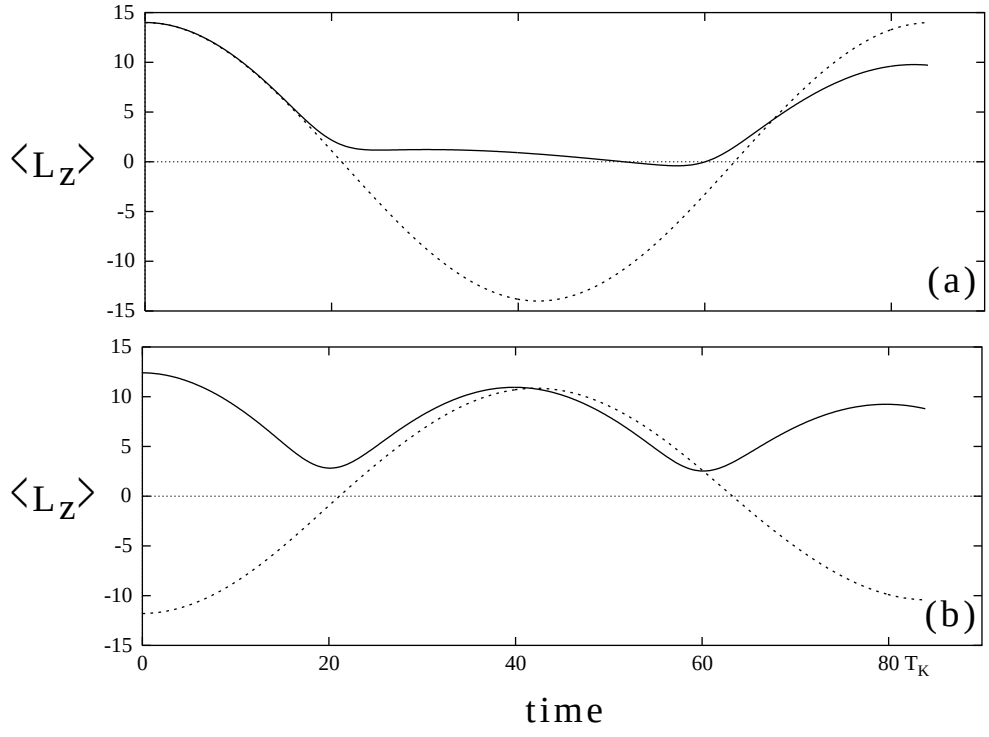

Figure 4: The quantum mechanical evolution of the expectation value of the z-component of the angular momentum for the wavefunction dynamics shown in the animations (Figs. 3 and 6). The evolution is followed for one Stark period. a) $\langle L_z(t) \rangle$ for the states shown in Fig. 3. The dashed curve is hydrogen and the solid curve is sodium. b) The evolution for core-scattered wave packets shown in Fig. 6. The dashed is the wave packet given initially by $m < 0$ states and the solid curve is the wave packet given initially by $m \geq 0$ states.

#1956 - $10.00 US
Received June 25, 1997; Revised July 3, 1997

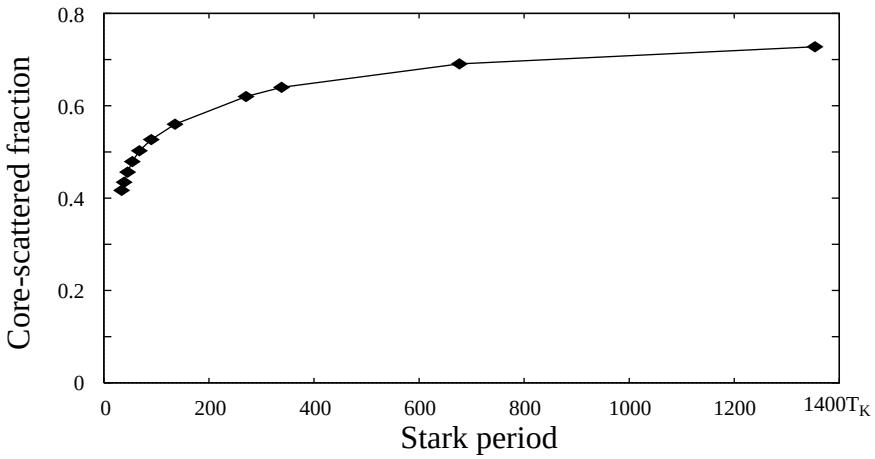

Figure 5: The ratio of the scattered wavefunction ($m > 0$) to the unscattered wavefunction ($m \leq 0$) is plotted as a function of the Stark period. Classically for larger Stark periods the electron spends more time in the low angular momentum orbit. Quantum mechanically this extended period of scattering leads to an increase in the scattered fraction of the wavefunction.

To examine core effects quantum mechanically we integrate Schrodinger's equation in a weak dc electric field using sodium dipole moments[18] for the $n = 15$ manifold. We also include the $16s$ and $16p$ states whose large quantum defects place them within the $n = 15$ manifold.

The animation in Fig. 3b shows the results of this calculation for an initial circular state. The behavior is initially hydrogenic but as the eccentricity increases we see evidence of the underlying classical precession. However, part of the wavefunction appears to continue to behave hydrogenically and after half of a Stark period these two parts of the wavefunction interfere in counter-propagating circular states. During the second collision with the core, the non-hydrogenic part of the wavefunction is rescattered and after one full Stark period the total wavefunction is almost entirely in the original circular state. The time dependence of the expectation value of the angular momentum (see Fig. 4a) behaves like neither hydrogen or classical sodium.

4. Stark dynamics of core-scattered wave packets

In order to understand the physics underlying this effect we will divide the wavefunction at $t = 0.5T_s$ into two wave packets: one containing only states for which $m < 0$ (this part of the wave function did not scatter from the core) and the other containing the remaining $m \geq 0$ states (this represents the scattered portion of the total wavefunction). Experimentally this could be accomplished through the use of selective field ionization of the wave packet at $t = 0.5T_s$.

Before renormalization, the total population in the $m < 0$ states was approximately 48% with the remaining 52% scattered into the $m \geq 0$ states. The ratio between the scattered and unscattered parts of the wave function varies as a function of the strength of the electric field. The dependence is approximately logarithmic on the Stark period as shown in Fig 5.

The reason for such a division of the wavefunction is revealed in the animations shown in Fig. 6. The behavior of the wave packets is strikingly different in the two cases.

#1956 - $10.00 US
Received June 25, 1997; Revised July 3, 1997

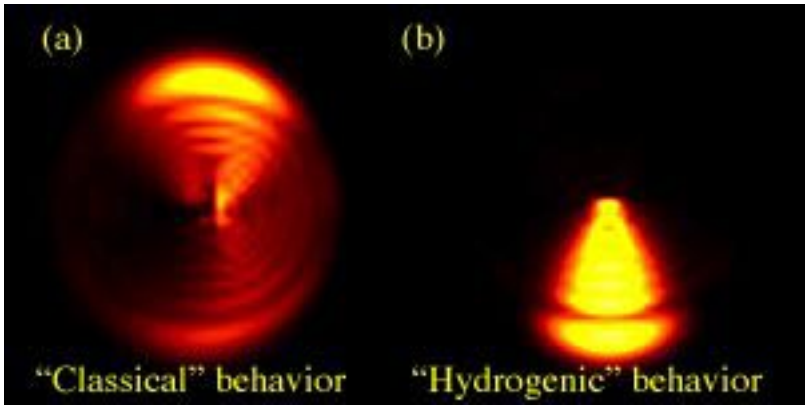

Figure 6: An animation comparing the quantum Stark dynamics of the core-scattered wave packet (initially $m \geq 0$ states) and the "hydrogenic" wave packet (initially $m < 0$ states). In both cases the dc electric field strength is 800 V/cm in the x-direction. a) This wave packet isolates the effect of core scattering and its behavior is very similar to the classical trajectory in Fig. 1b. b) Interference near the core minimizes core scattering and leads to nearly hydrogenic behavior.

The $m < 0$ wave packet in Fig. 6b behaves nearly hydrogenically except near the core where, unlike hydrogen, there is never appreciable population. Because of this interference near the core the $m < 0$ wave packet experiences much reduced core scattering resulting in hydrogenic behavior. The wave packet consisting of $m \geq 0$ states displays the rapid precession characteristic of the classical sodium model and is almost entirely scattered from the core. As in the classical model, this scattering process lasts only a few Kepler periods as the wavefunction precesses by approximately 180°.

In Fig. 4b we show the evolution of the angular momenta of the two wave packets discussed above. The difference in the scattering behavior is clearly evident and shows all of the features of the classical behavior shown in Fig. 2. The the finite extent of the quantum wave function smoothes the minima of the angular momentum of the scattered wave packet. We also see the shortening of the Stark period in the scattered case.

5. Summary

We have presented a classical perspective of core-scattering in alkali atoms by using the Stark dynamics of angularly localized wave packets to visualize core effects. Although the scattering of these wave packets has a classical interpretation there is not a direct correspondence between the classical and quantum theories as there is in hydrogen. The phase shifts associated with the quantum defects of the low angular momentum alkali states produce interference which leads to behavior containing features of both classical sodium and classical hydrogen. The use of angularly-localized wave packets reveals how quantum phase affects the dynamics underlying scattering and allows us to understand the behavior suggested by the studies of semiclassical scaled energy spectra.

6. Acknowledgments

We would like to acknowledge Z. D. Gaeta and J. Bromage for useful discussions, and the Army Research Office for support of this research.

#1956 - $10.00 US
Received June 25, 1997; Revised July 3, 1997